Idaho National Engineering Laboratory

Managed by the U.S. Department of Energy

EGG-NE-8940
April 1990

REACTIVITY STUDIES ON THE FINAL PRECONCEPTUAL REFERENCE DESIGN OF THE ADVANCED NEUTRON SOURCE

J. M. Ryskamp, E. L. Redmond II, S. S. Kim, and C. D. Fletcher

EG&G Idaho

Work performed under DOE Contract No. DE-AC07-76ID01570

EGG-NE--8940

DE90 013098

REACTIVITY STUDIES ON THE FINAL PRECONCEPTUAL REFERENCE DESIGN OF THE ADVANCED NEUTRON SOURCE

J. M. Ryskamp, E. L. Redmond II, S. S. Kim, and C. D. Fletcher

Idaho National Engineering Laboratory
EG&G Idaho, Inc.
P. O. Box 1625
Idaho Falls, ID 83415-3515

April 1990

Work performed under the auspices of the U. S. Department of Energy
Under DOE Contract No. DE-AC07-76ID01570.

ABSTRACT

An Advanced Neutron Source (ANS) with a peak thermal neutron flux of 8.0-9.0 x 10^{19} $m^{-2}s^{-1}$ is being designed for condensed matter physics, materials science, isotope production, and fundamental physics research. A final preconceptual reference reactor design has been selected in order to examine the safety, performance, and costs associated with this one design. This report presents reactor physics analyses of safety aspects of the reference reactor design that are related to core reactivity changes. These analyses include control rod worth, shutdown rod worth, heavy water voiding, light water ingress, single fuel element criticality, fuel element movement, and neutron beam tube flooding. The positive and negative findings are explored for each of these analyses. Based on these analyses, some design modifications that further improve the reactor safety are identified and recommended.

SUMMARY

Reactor physics analyses of safety aspects related to core reactivity changes have been conducted on the final preconceptual reference design of the Advanced Neutron Source. These analyses include control rod worth, shutdown rod worth, heavy water voiding, light water ingress, single fuel element criticality, fuel element movement, and neutron beam tube flooding. The positive and negative findings for each of these analyses are summarized in Table 1. Understanding these safety aspects will allow us to make design modifications that improve the reactor safety and achieve the safety related design criteria. In addition, these results are being used for transient analyses that will increase our knowledge of the ANS accident response and lead to further safety enhancement.

TABLE 1. MAJOR FINDINGS FROM REACTIVITY STUDIES ON THE FINAL PRECONCEPTUAL REFERENCE DESIGN OF THE ADVANCED NEUTRON SOURCE

Subject	Positive Finding	Issues Identified
Control rod worth	Reactor can be controlled with shim rods in the central hole; adequate shutdown margin exists.	Rods have high neutron and gamma heating rates and will be difficult to cool in current configuration.
Shutdown rod worth	Reactor can be shut down with shutdown rods only; adequate shutdown margin exists.	Shutdown rods in the reflector tank need to be tilted slightly, making exact calculations difficult.
Heavy water voiding	Heavy water voiding in nearly all regions decreases the core reactivity.	Voiding in the coolant bypass annulus slightly increases the core reactivity.
Light water ingress	Light water ingress decreases the core reactivity in all regions except the coolant channels.	Light water ingress into the coolant channels increases the core reactivity.
Single fuel element criticality	Each fuel element is subcritical when dropped into a large pool of light water.	Each fuel element is supercritical when dropped into a tank of heavy water.
Fuel element movement	Movement (or collapse) of fuel elements to the axially aligned position reduces the core reactivity.	Movement (or collapse) of fuel elements towards each other initially increases the core reactivity.
Neutron beam tube flooding	Flooding of one beam tube will not result in a major reactivity increase.	Flooding of several beam tubes simultaneously could result in a significant reactivity increase.

CONTENTS

TABLES

TABLES (CONTD)

FIGURES

1. INTRODUCTION

An Advanced Neutron Source (ANS) with a peak thermal neutron flux of about 8.0-9.0 x 10^{19} $m^{-2}s^{-1}$ is being designed for condensed matter physics, materials science, isotope production, and fundamental physics research. The ANS is a new reactor-based research facility being planned by Oak Ridge National Laboratory (ORNL) to meet the need for an intense steady-state source of neutrons.[1,2] The design effort is currently in the conceptual phase. The final preconceptual reference reactor design has been selected in order to examine the safety, performance, and costs associated with this one design.[3] The ANS Project has an established, documented safety philosophy, and safety-related design criteria are currently being established.[4]

The purpose of this report is to present the reference reactor physics analyses of safety aspects of the reference reactor design that are related to core reactivity changes. These analyses include control rod worth, shutdown rod worth, heavy water voiding, light water ingress, single fuel element criticality, fuel element movement, and neutron beam tube flooding. Understanding these safety aspects will allow us to make design modifications that improve the reactor safety related design criteria. In addition, these results are being used for transient analyses that will increase our knowledge of the ANS accident response and lead to further safety enhancement.

The reference reactor consists of two fuel elements containing hundreds of thin involute fuel plates with highly-enriched uranium silicide (U_3Si_2) fuel meat.[3] As shown in Figure 1, the elements are radially and axially offset. Thus we call this the offset split core design. Radially offset fuel elements allow the same low coolant inlet temperature for each element. This greatly improves the thermal hydraulic safety margins over an aligned concept in which the heated coolant out of the first element flows into the second element. The fuel elements are offset axially to create greater neutron leakage, which increases the volume of the reflector that experiences a high thermal neutron flux. The neutron and gamma heating effects on reactor and reflector components are smaller

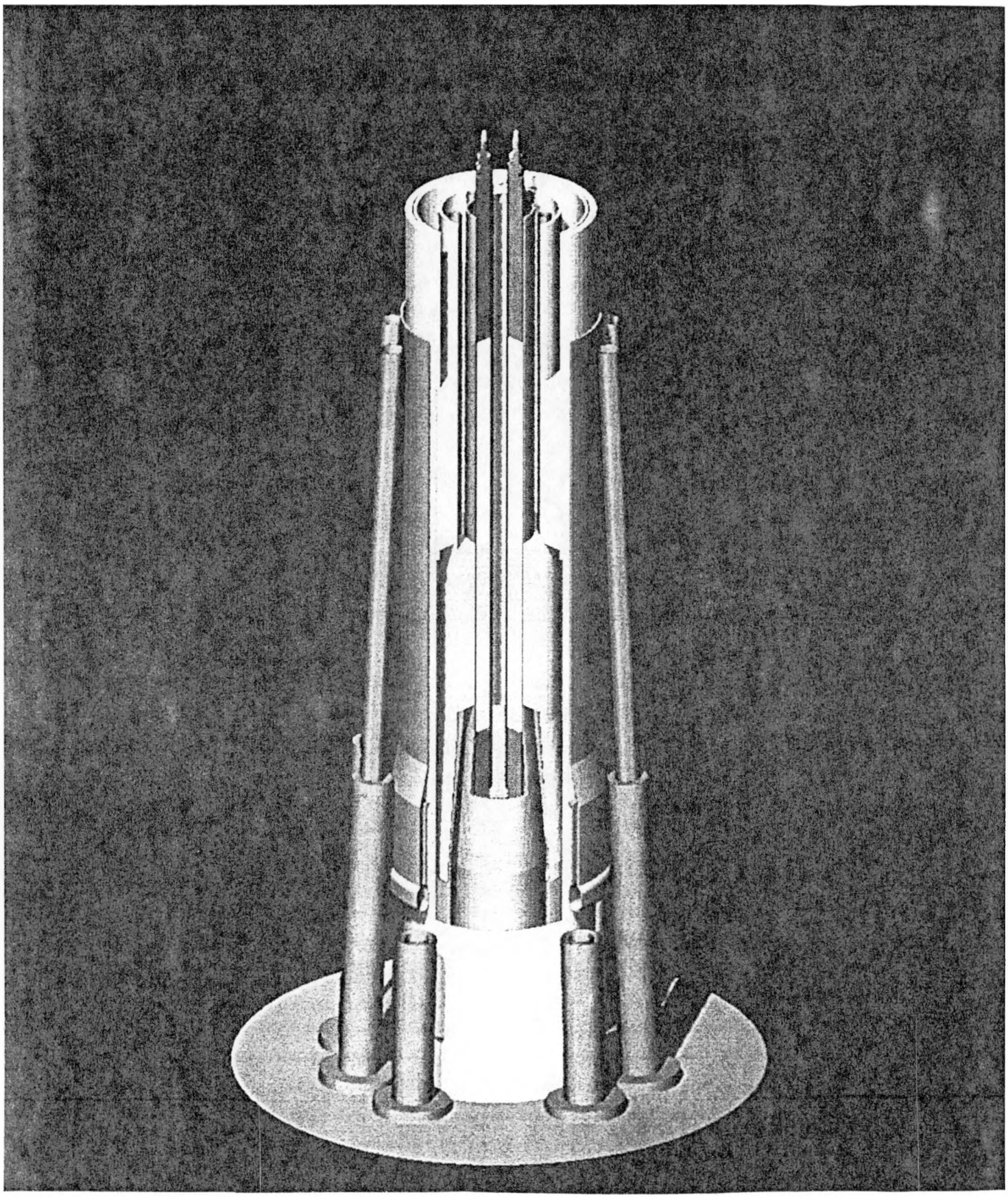

Figure 1. The Advanced Neutron Source reference offset split core with involute fuel plates.

with axially separated fuel elements. This configuration also increases the available worth of the control rods in the central hole region and provides additional space next to the fuel for irradiation targets.

The entire reactor and core pressure boundary tube (CPBT) are surrounded by a large, low-pressure and low-temperature tank of heavy water. Because fast neutrons produced in the fuel leak through the CPBT, the thermal neutron flux peaks outside the reactor in the reflector tank. Heavy water in this region slows the neutrons to thermal energies (< 1 eV). Beam tubes placed in the tank will permit access to the resulting high flux environment with minimum high-energy-neutron and gamma contamination from the core. The D_2O reflector is contained in a large, 3.5-m-diameter, Al-6061 vessel surrounded by H_2O. The light water pool provides biological shielding.

The characteristics of the reference reactor are presented in Table 2. The reactor operates for 14 days at a power of 350 MW-fission to achieve a peak thermal neutron flux of about 8.5×10^{19} $m^{-2}s^{-1}$ in the reflector at the end of cycle (EOC). The fuel meat is highly enriched (93% U-235) U_3Si_2/Al, 0.762-mm-thick, and is clad with 0.25-mm-thick Al-6061. The U-235 loading varies continuously, axially and radially, throughout the fuel to reduce the local power peaking. Burnable boron poison is provided in the end caps of the fuel to reduce the excess reactivity at the beginning of cycle and to help flatten the power distribution. The plates are cooled with D_2O flowing up 1.27-mm-wide coolant channels. The upper element has 432 involute fuel plates containing a total of 9.36 kg U-235; the lower element has 252 plates with 5.65 kg U-235. The involute plates are welded to cylindrical Al-6061 side plates, similar to the High Flux Isotope Reactor (HFIR) fuel elements. Heavy water flowing through a coolant bypass annulus between the outer side plates and the CPBT cools the side plates and CPBT.

A shim/regulating/safety control rod system is located in the central hole, and a safety control rod system is located in the reflector just

TABLE 2. DESIGN CHARACTERISTICS OF THE REFERENCE OFFSET SPLIT CORE MODEL

Core Dimensions	
Fuel element height (mm)	474
with Al end tips	494
Upper fuel element	
Inner diameter (mm)	350
Outer diameter (mm)	482
Radial thickness (mm)	66
Lower fuel element	
Inner diameter (mm)	204
Outer diameter (mm)	336
Radial thickness (mm)	66
Core volume (litres)	67.42
Core total height (mm)	1038
Volume of fuel meat (litres)	20.23
Axial distance between active fuel elements (mm)	50
Coolant bypass annulus width (mm)	5
Al-6061 core pressure boundary tube thickness (mm)	12.5
Al-6061 central support pipe thickness (mm)	7.0
Fuel plate surface area in core (m^2)	53.0
Central hole diameter (mm)	190
Fuel	
Material	U_3Si_2/Al
Uranium enrichment (weight % U-235)	93
Maximum volume fraction (U in fuel meat)	0.45
Maximum fuel density (kg U/L fuel meat)	2.25
Fuel plate thickness (mm)	1.27
Coolant channel width (mm)	1.27
Fuel meat thickness (mm)	0.76
Cladding and side plate material	Al-6061
Cladding thickness (mm)	0.254
Al-6061 plate tip length (mm)	10.0
Number of fuel plates	
Upper element	432
Lower element	252
Total 684	
Side plate thickness (mm)	7.0
Fuel span between side plates (mm)	
Upper element	78.4
Lower element	87.4
Fuel volume fraction in core	0.30
Coolant volume fraction in core	0.50
Cladding volume fraction in core	0.20

TABLE 2 (CONTINUED)

Physics Characteristics

Reactor power (constant) (MW-fission)	350.0
(MW-core)	332.5
Cycle length (days at full power)	14.0
Core average power density (MWf/L)	5.19
Peak reflector thermal neutron flux,	
$E < 0.625$ eV ($m^{-2}s^{-1}$) Beginning-of-cycle	7.95×10^{19}
Middle-of-cycle	8.37×10^{19}
End-of-cycle	8.57×10^{19}
Fast neutron ($E > 0.1$ MeV) contamination at thermal flux peak location at BOC ($m^{-2}s^{-1}$)	7.95×10^{17}
Core fissile loading at BOC (kg U-235)	15.01
Fuel burnup (kg U-235)	6.07
average (fissions/m^3 meat)	6.3×10^{26}
peak (fissions/m^3 meat)	1.0×10^{27}
Core burnable poison loading (kg B^{10}) at BOC	0.0134
Core burnable poison loading (kg B^{10}) at EOC	0.0002
Maximum k excess (%$\Delta k/k$)	24.2
Efficiency factor at EOC ($m^{-2}s^{-1}$ MWf^{-1})	2.45×10^{17}
Axial distance of thermal flux peak relative to core midplane	
at BOC (m)	-0.15
at EOC (m)	0.07
Radial distance of thermal flux peak	
at BOC (m)	0.38
at EOC (m)	0.38
Fast-to-thermal flux ratio at flux peak at EOC at location of peak thermal flux	0.010

Fluxes at Target Irradiation Positions at BOC

Group energy boundaries

Group 1 (fast)	0.1 MeV < E < 17 MeV
Group 2	100 eV < E < 0.1 MeV
Group 3 (epithermal)	0.625 eV < E < 100 eV
Group 4 (thermal)	0.0 eV < E < 0.625 eV

Fast flux irradiation position - above lower element
152 mm < r < 168 mm

Average group 1 flux ($m^{-2}s^{-1}$)	3.58×10^{19}
Average group 2 flux ($m^{-2}s^{-1}$)	5.37×10^{19}
Average group 3 flux ($m^{-2}s^{-1}$)	1.88×10^{19}
Average group 4 flux ($m^{-2}s^{-1}$)	1.05×10^{19}

Epithermal flux irradiation position-below upper element
175 mm < r < 193 mm

Average group 1 flux ($m^{-2}s^{-1}$)	2.88×10^{19}
Average group 2 flux ($m^{-2}s^{-1}$)	4.35×10^{19}
Average group 3 flux ($m^{-2}s^{-1}$)	1.79×10^{19}
Average group 4 flux ($m^{-2}s^{-1}$)	3.08×10^{19}

TABLE 2 (CONTINUED)

Thermal flux irradiation position - at r = 1.5 m in tank	
Average group 1 flux ($m^{-2}s^{-1}$)	~2 x 10^{10}
Average group 2 flux ($m^{-2}s^{-1}$)	~3 x 10^{12}
Average group 3 flux ($m^{-2}s^{-1}$)	~5 x 10^{14}
Average group 4 flux ($m^{-2}s^{-1}$)	~4 x 10^{18}
Thermal Hydraulic Conditions	
Coolant inlet pressure (MPa)	3.7
Core outlet pressure (MPa)	2.0
Core pressure drop (MPa)	1.7
Available flow area (m^2)	
in upper element coolant channels	0.0431
in lower element coolant channels	0.0280
in coolant bypass annulus	0.00787
in control rod channel	0.025
Coolant flow rate (kg/s)	
in upper element coolant channels	1196
in lower element coolant channels	770
in coolant bypass annulus	129
in control rod channel	274
Coolant velocity (m/s)	
in core channels	27.4
in coolant bypass annulus	15.0
in control rod channel (new value = 15.0)	10.0
Coolant bulk inlet temperature (^oC)	49
Coolant bulk outlet temperature (^oC)	83
Average surface heat flux (MWc/m^2)	6.27
Average heat transfer area per plate	
upper element (m^2)	0.0743
lower element (m^2)	0.0828
Energy conversion factor (%)	
(MW-core/MW-fission)	95.0
Average power density in fuel meat (MWc/L)	16.44

outside the CPBT. Approximately 20% $\Delta k/k$ excess reactivity is required at the beginning of cycle (BOC) to maintain a reactor power of 350 MWf for 14 days. About 11% of the core excess reactivity at the beginning of cycle is shimmed with 13.4 g of burnable boron poison. The remaining excess reactivity at BOC is controlled by four hafnium rods in the central hole.

The high power densities require a reasonably flat power distribution. The power shape is flattened by burnable boron poison and by

grading the fuel, radially and axially, placing higher U-235 content near the center of the fuel zone and lower U-235 content in the core periphery. Each involute plate in either element has the same U-235 distribution as the other plates in that element.

The region of peak thermal neutron flux occurs in the D_2O reflector about 120 mm outside the core pressure boundary tube, covering a large volume, which also has low fast-neutron and gamma-ray contamination. Figure 2 is a radial flux plot at the axial location of the peak thermal neutron flux. The group energy boundaries are listed in Table 2. The fast neutron and gamma contamination drops off rapidly with radial distance.

2. ANALYTICAL METHODOLOGY

Reactor physics analyses were performed with ENDF/B-V cross section data. Many of the methods we used are well documented.[5] We processed 28-group cross section libraries with the COMBINE[6] code using the calculated flux and current spectra from different unit cells as weighting functions. We used one-dimensional (1D) cylindrical transport models (SCRABL) to collapse cross sections to four groups. These models were iterated with two-dimensional (2D) four-group diffusion theory calculations to make sure the axial leakage in each group was estimated correctly for the 1D transport model.

Four-group cross sections were calculated in different regions. In particular, the one-thermal-group U-235 capture and fission cross sections vary significantly depending on the distance from the core periphery. This occurs because the flux spectra are very hard in the center of each fuel element, but are considerably softer in the fuel regions adjacent to the heavy water. Spatially-dependent cross sections permit the use of inexpensive computations using one thermal group and three fast groups. Additional thermal groups reduce the need for spatially-dependent cross sections, but increase computer costs because the treatment of neutron upscattering in the thermal range requires an iterative procedure.

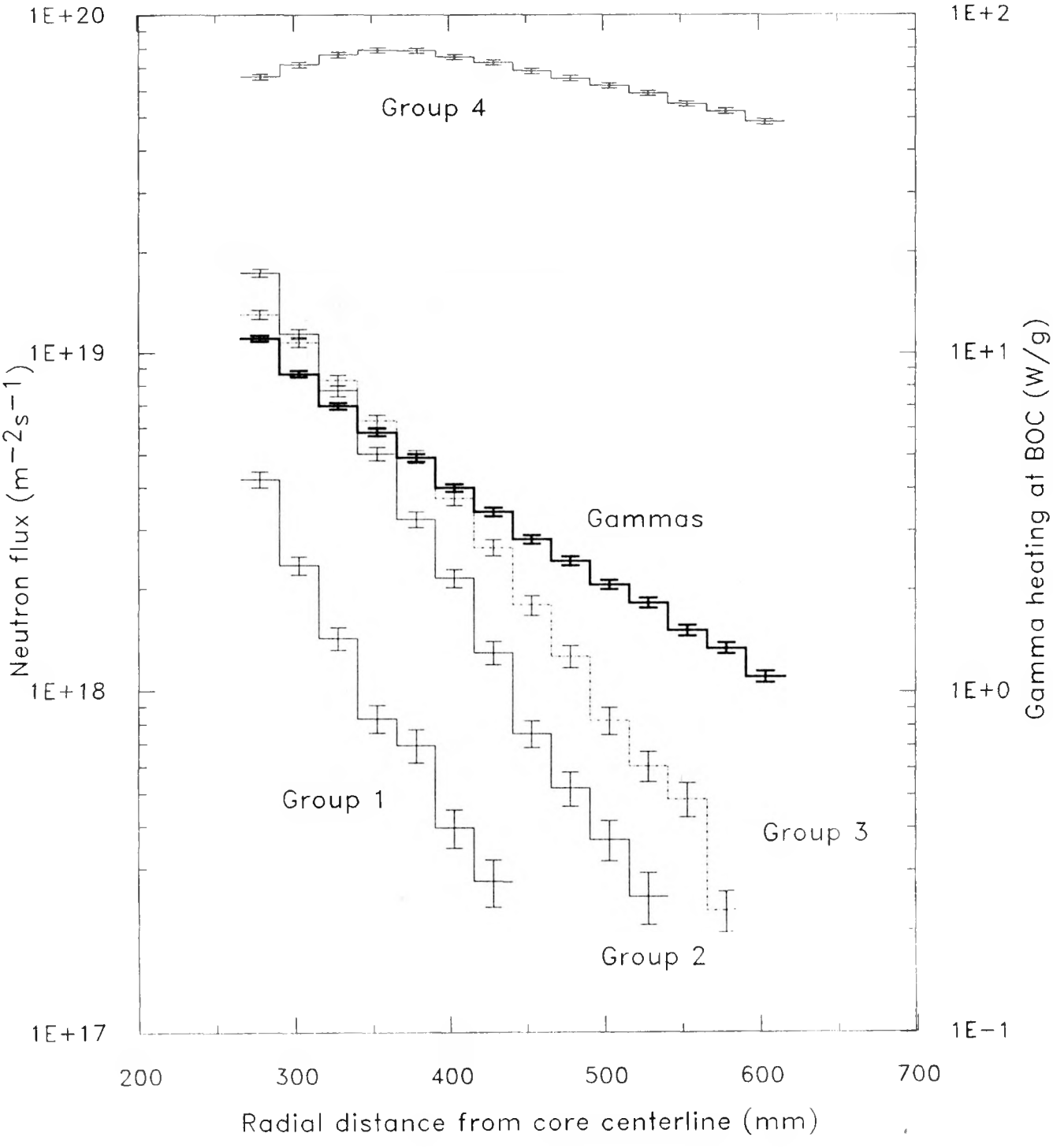

Figure 2. Neutron fluxes and gamma heat versus radial distance along the axial location of the peak thermal neutron flux at BOC. The MCNP-generated values are between 143 mm and 203 mm below the core midplane.

Some of the reactor physics calculations were performed with PDQ-7[7] using two-dimensional, four-energy-group, diffusion theory models. Other calculations were performed with MCNP-3B[8] using three-dimensional, continuous-energy, Monte Carlo theory models. The fuel was modeled with 160 regions. This is a reasonable way to represent the continuously-graded, highly-enriched uranium silicide fuel. The mesh structure in the PDQ-7 model was examined and modified to account for the very steep flux gradients near the fuel-water interface. The geometry and composition of the PDQ-7 and MCNP-3B models are nearly identical. However, control rods, shutdown rods, and beam tubes are represented in full detail in the three-dimensional MCNP-3B model.

The MCNP-3B model is currently the most sophisticated and accurate neutronics model of the ANS and is being used as a benchmark to compare with other calculations.[9,10] The disadvantage is that two to five hours of CRAY time are required to solve each problem within adequate statistics. The MCNP calculations are generally much more accurate, as well as much more expensive, than the PDQ calculations. The MCNP models were used in cases where three dimensions are required (such as for beam tubes or control rods) or where diffusion theory is inadequate (such as for large voids). PDQ models were used for the remaining cases and when the reactivity changes are very small, since the statistical nature of Monte Carlo prohibits examining small differences.

Some thermal hydraulic analyses were performed with RELAP5/MOD3, an advanced version of RELAP5/MOD2.[11] RELAP5 was used to compute a large break loss-of-coolant accident simulation, which is representative of core voiding, and therefore coolant density response, during depressurization accidents.[12]

3. CONTROL AND SHUTDOWN ROD WORTHS

Four hafnium control rods in the central hole are represented explicitly in the three-dimensional MCNP model. They are homogenized in the central hole of the PDQ r-z model. MCNP also accurately models the eight reflector shutdown rods surrounding the reactor. Table 3 presents

the core multiplication factors for different central control rod bank and reflector shutdown rod bank positions. A graded fuel core model containing boron in the end caps was used for these studies. These results indicate that the current configuration of four control rods in the central hole is adequate to shut down the reactor. The control rods also have negligible reactivity effect when in the fully withdrawn position. The reactor is near critical when the control rod bank is at the core midplane. The reflector shutdown rods are capable of safely bringing the ANS to a subcritical state even with the control rods fully withdrawn.

TABLE 3. CENTRAL CONTROL ROD BANK WORTH AND REFLECTOR SHUTDOWN ROD BANK WORTH AT BEGINNING OF CYCLE

Description	Core Multiplication Factor	
	PDQ	MCNP[a]
Base Case - No control rods	1.1490	1.1205 ± 0.0045
Control rods fully withdrawn (100 mm above top element)		1.1162 ± 0.0040
Control rods fully inserted	0.9375	0.9014 ± 0.0032
Control rods inserted to core midplane	1.0236	1.0036 ± 0.0040
Reflector shutdown rods fully inserted with no control rods		0.8568 ± 0.0030

a. The statistical uncertainties reported with all MCNP calculations represent one standard deviation.

A comparison of the change in the core multiplication factor as calculated by PDQ and MCNP for control rods inserted to core midplane indicates that PDQ does a good job of estimating the control rod bank worths even though PDQ cross sections are homogenized over the central hole. PDQ-7 predicts a reactivity change of -11.6%, and MCNP-3B predicts a reactivity change of -11.0%. These values represent the effect of placing control rods inserted to core midplane in a model that did not previously contain control rods.

Gamma and neutron heating in the four control rods is significant[9,10] and must be considered when selecting the control rod design. Control rod geometries with greater surface-to-volume ratios may be easier to cool.

4. HEAVY WATER VOIDING

MCNP and PDQ were used to determine the effects of voiding heavy water regions on the core multiplication factor. Table 4 lists the results of these calculations. Diffusion theory is not accurate in highly voided regions. However, diffusion theory can identify the general magnitude and the sign of the reactivity changes, as shown by comparing the last two columns of numbers in Table 4.

For example, completely voiding all coolant channels shifts the flux spectrum in the fuel to faster neutron energies, making the flux spectrum harder. This changes the U-235 cross sections that are used in the MCNP model. However, the PDQ runs used the same U-235 cross sections as the base case with heavy water. PDQ may have given better answers if funding had been provided to recompute the cross sections for different cases.

In all regions, the appearance of void decreases reactivity, except in the coolant bypass annulus, where there is small positive reactivity insertion. Voiding the coolant channels results in a negative reactivity insertion because the fuel elements are very undermoderated. Voiding at the coolant exits in the upper plenum decreases reactivity, so the most likely cause of voiding, steam generated in the fuel elements, has a negative effect on core reactivity. Voiding in the central hole also decreases reactivity, even with control rods inserted to core midplane. Thus, the flux spectrum does not shift enough to significantly reduce the worth of the control rods. This may be partially because the hafnium nuclides in the rods have high epithermal cross sections as well as high thermal cross sections. The rods are very black over a wide neutron energy range.

TABLE 4. EFFECTS OF D_2O VOIDING ON THE CORE REACTIVITY

Voided Region	Region Volume (L)	Core Reactivity Change (%) MCNP	PDQ
Coolant channels without control rods	33.71	-4.98	-2.74
Coolant channels with control rods above midplane	33.71		-3.29
Plenum above lower fuel element without control rods	18.91	-2.19	-2.96
Plenum below upper fuel element with control rods above midplane	41.00		-0.55
30 mm of void above upper fuel element without control rods	2.82		-0.28
Central hole with control rods above midplane	109.9	-5.98	
Central hole without control rods	113.9		-3.36
Central hole below midplane with control rods above midplane	56.96		-3.65
Coolant bypass annulus without control rods	3.81		+0.22
with rods above midplane	3.81		+0.17
10% void in entire reflector tank with control rods above midplane	38456.0		-2.10

a. The statistical uncertainties of the MCNP calculations are typically $\pm$0.004 for one standard deviation of the core multiplication factor.

There is a small positive reactivity insertion when voiding the bypass annulus. MCNP could be used to check this value. However, the statistical fluctuation may be larger than the difference between the computed core multiplication factors. ORNL has performed some one-dimensional transport theory calculations that confirm there is a positive reactivity insertion with voiding in the bypass annulus. Voiding the annulus removes the moderator just outside the fuel. This produces a harder flux spectrum

passing out through the core pressure boundary tube (CPBT). Thus fewer neutrons are captured in the CPBT and more leak into the reflector where they slow down. The core reactivity increases slightly.

If the coolant bypass annulus was wider, the effect could be worse. However, eventually when it is wide enough, the reactivity would drop with voiding because the CPBT would be worth less. This was confirmed by voiding the wide plenum region below the upper fuel element. When selecting the bypass width, designers must be careful not to make the width too small just because of the voiding problem. With a very small width, there may not be enough heavy water to cool the outer fuel element side plate and CPBT during an accident. This would increase the likelihood of voiding in the bypass annulus, even though the reactivity consequences would be very small. A larger bypass annulus may prevent significant voiding from ever occurring.

Voiding the D_2O completely in the central hole reduces the core reactivity, with or without control rods present. PDQ-7 and MCNP both showed negative void coefficients of about the same magnitude. Here we verify that partial voiding in the central hole also reduces the core reactivity. PDQ-7 calculations of the core reactivity drop are listed in Table 5. No control rods are present, and only the portion of the central hole that is adjacent to the fuel elements is voided. Partially voiding just the portion of the central hole adjacent to the upper fuel element also decreases the core reactivity.

TABLE 5. THE EFFECT OF PARTIAL HEAVY WATER VOIDING IN THE CENTRAL HOLE ON THE CORE REACTIVITY

Percent of Void	Percent Reactivity Change from 0% Void
10	-0.251
20	-0.523
100	-3.364

TABLE 6. VOID COEFFICIENTS OF REACTIVITY IN DIFFERENT REGIONS

Voided Region	Void Coefficient (%ρ/liter of void)	Void Coefficient ($/liter of void)
Coolant channels	-0.148	-0.206
Plenum above lower fuel element	-0.116	-0.161
Plenum below upper fuel element	-0.013	-0.018
Plenum just above upper fuel element	-0.099	-0.137
Central hole	-0.054	-0.075
Coolant bypass annulus	+0.058	+0.081
Reflector tank	-0.00055	-0.00076

The void coefficients of reactivity in different regions are listed in Table 6. These were computed using the data in Table 4, with the MCNP values preferred over the PDQ values. The delayed neutron fraction was assumed to be 0.0072 to compute the worth in dollars (this becomes about 0.008 when photoneutrons are included). The void coefficients are most negative in the coolant channels and in the plenum above the lower fuel element. Voiding the entire coolant bypass annulus leads to a positive 0.31$ reactivity insertion.

The rod worths and void coefficients are being used in RELAP5 to analyze several accident scenarios. The Advanced Neutron Source core region fluid density response expected during a representative accident was developed for use as boundary condition data in ANS reactivity studies. A system model of the ANS final preconceptual design implemented in the RELAP5/MOD3 computer code has been used to perform preliminary simulations of large, medium, and small break loss-of-coolant accidents (LOCA). The end point of the large break loss-of-coolant accident simulation was selected as representative of core voiding, and therefore core density response, during depressurization accidents. The calculation simulated the complete rupture of a pump discharge pipe in one heat

exchanger loop; the break flow area was 0.08317 m^2. Density changes resulted from fluid voiding, compressibility, and thermal effects. The conditions at the end of the calculation likely include a maximum expected core voiding with the core geometry remaining intact. The RELAP5 point kinetics model is driven by component reactivities resulting from changes in fluid temperature, and the scram rod position. Preliminary results indicate that a loss of coolant accident reduces core reactivity.

5. LIGHT WATER INGRESS

The core reactivity depends on the type of moderator present. Light water moderates neutrons much faster and in a much shorter distance than heavy water. However, light water also absorbs more neutrons than heavy water. The ANS was designed specifically to take advantage of the properties of heavy water. The reactor is cooled and moderated by heavy water and is immersed in a large tank of heavy water surrounded by a light water pool. Light water ingress into the reactor or heavy water tank is a very unlikely event, but is thought to be possible for some accident scenarios. Detailed evaluations of the probability of light water ingress have not yet been performed. The reactivity impact of light water ingress has been examined.

The four-group diffusion theory code PDQ-7 is used to analyze two-dimensional (r-z) models of the offset split core. The four-group cross sections for all materials were obtained previously by collapsing cross sections over appropriate flux spectra with D_2O present. Because the presence of light water shifts the flux spectra, we recomputed the light water cross sections in different regions. The H_2O cross sections changed significantly (these can change the calculated core multiplication factor by as much as 7%). Other cross sections will also change somewhat, but were not recomputed because of the limited time available to perform this task. So, some uncertainty exists in the core multiplication factors because all cross sections were not recomputed, but we expect that this uncertainty is much less than the calculated reactivity impact due to the light water.

Table 7 shows the reactivity impact of substituting H_2O for D_2O in different regions inside the core pressure boundary tube. Light water ingress in most regions reduces the core reactivity. One safety concern is that of an isolated slug (or slugs) of light water within the heavy water stream entering the fuel region. If two optimally shaped slugs that are offset both axially and radially enter each fuel element at the same time (an incredible scenario) and displace all of the heavy water in the coolant channels, but not in the bypass annulus, there would be a pulse of positive reactivity insertion of about 15$ in about 0.02 seconds, under present ANS design conditions. This pulse is quickly preceeded and followed by reactivity drops. We have been unable to identify any credible mechanism by which two separate, unmixed, unaligned slugs of light water could enter the high pressure heavy water system during normal operation without triggering a reactor scram. In reality the two slugs in the separate flow paths would most likely be aligned axially, partially mixed, and not of optimum shape. In addition, the primary coolant flow is much greater than potential injection flows by a factor of 30 to 100.

TABLE 7. REACTIVITY IMPACT OF LIGHT WATER INGRESS IN THE ADVANCED NEUTRON SOURCE AT BEGINNING OF CYCLE WITH ALL RODS FULLY WITHDRAWN AND NO BURNABLE BORON POISON

Regions with H_2O Inside CPBT	Core Multiplication Factor (k)	Reactivity Impact (%Δk/k)
None (no B-10 or Hf)	1.3118	--
All regions inside CPBT	1.0261	-24.6
All regions except D_2O in central hole	1.2350	- 6.0
Fuel regions only[b] (coolant channels)	1.4521	10.2

a. These are the regions inside the core pressure boundary tube (CPBT) where D_2O has been entirely replaced by H_2O. All models have D_2O in the reflector tank.
b. Figure 3 emphasizes how difficult it would be for two light water slugs to exist in both fuel elements simultaneously while being surrounded by heavy water in all other regions.

We have also investigated a more physically realizable scenario of a front of light water as it enters the core from the cold leg during full-power operation and progresses through the core, as shown in Figure 3. To provide boundary condition data for reactivity studies, a simple analysis was performed to evaluate the hydraulic response of the ANS heavy-water-cooled core to a sudden ingress of light-water. The analysis consisted of tracking the light/heavy-water interface through the three flow paths from the core inlet to the lower core, upper core, and central hole regions.

This analysis includes several simplifying assumptions and underlying uncertainties. The light/heavy-water interface is assumed to be well-defined, non-degrading, and flat as the interface passes upward through each of the three flow paths. In reality, the flow regime is highly turbulent and the propagation of a well-defined interface seems unlikely; however, this assumption results in step changes that likely overstate the actual change rates. The flat velocity profile function is likely adequate since for a turbulent flow the velocity gradients are confined to small boundary layers on the region walls. The central hole region is assumed to have a constant flow area throughout (representing a cylindrical tube containing the control rods). There is uncertainty in the flow velocity in the upper core bypass path between the outer side plate and the inside of the core pressure boundary tube. No attempt has been made to account for effects resulting from differences in light- and heavy-water fluid properties. Examples of these effects include the variation in frictional flow loss (due to changes in fluid density) and variation in fluid temperatures (due to changes in fluid specific heat).

Despite these uncertainties, we believe the simple analysis performed accounts for the most important hydraulic phenomena of a light-water ingress event. Coolant velocities of 27.4 m/s between the fuel plates, 15 m/s in the upper core bypass region, and 10 m/s in the central (control rod) hole region were assumed. Table 8 summarizes the assumed flow lengths and velocities in each flow region.

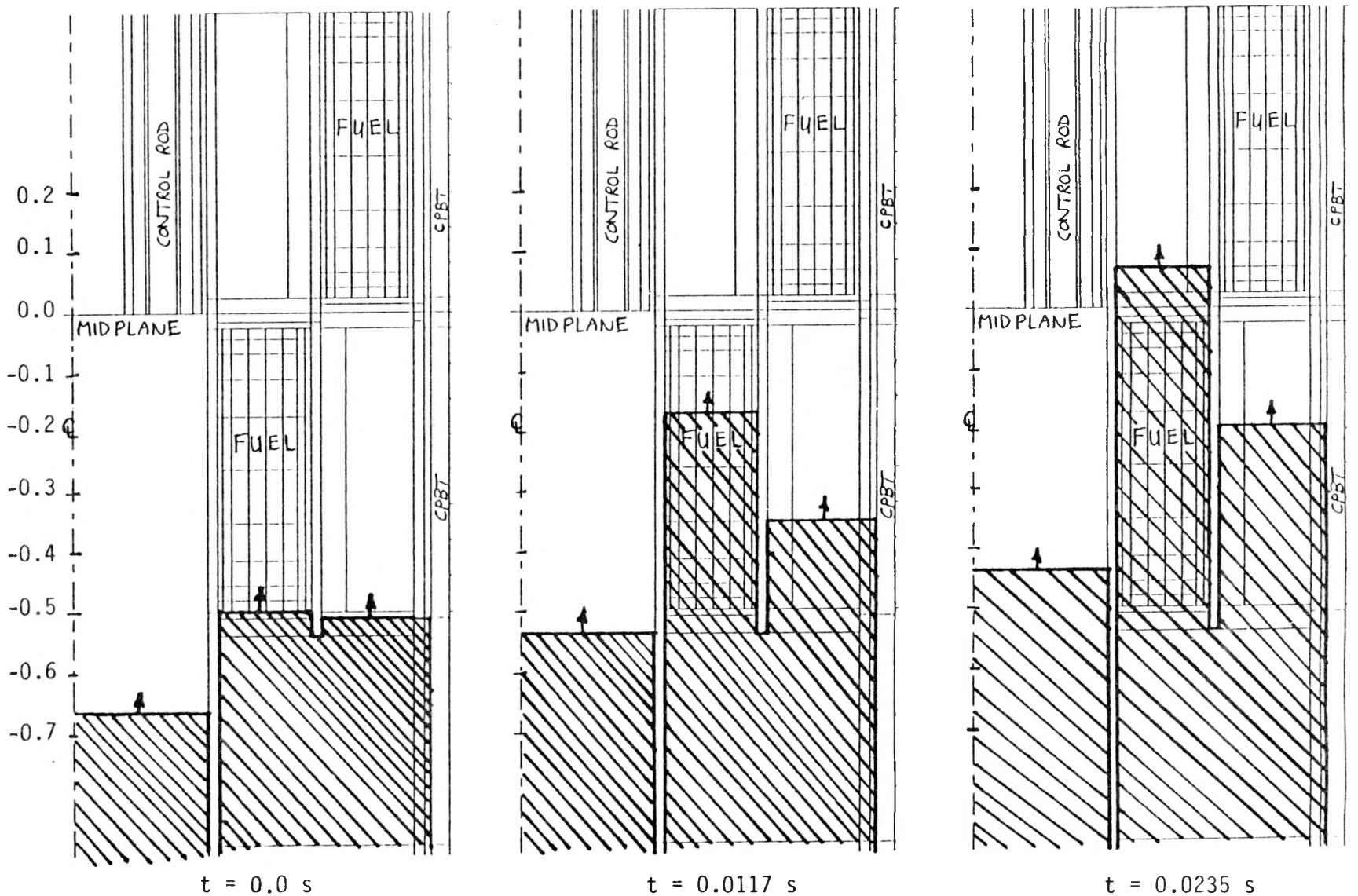

Figure 3. Progression of a front of light water as it enters the core from the cold leg during full-power operation. Heavy water has been replaced with light water in the cross-hatched regions.

TABLE 8. REGION LENGTHS AND FLOW VELOCITIES

Region	Length (m)	Velocity (m/s)
Lower Core Inlet	0.881	12.5
Lower Core	0.474	27.4
Inner Middle Plenum	0.050	12.8
Lower Core Outlet	1.678	12.8
Upper Core Inlet	1.355	12.4
Outer Middle Plenum	0.050	12.4
Upper Core	0.474	27.4
Upper Core Bypass	0.474	15.0
Upper Core Outlet	1.678	13.7/15.0[a]
Central Hole	3.083	10.0

a. A velocity of 13.7 m/s was used in the portion of this region above the heated core and 15 m/s was used in the portion of this region above the outer side plate-to-core pressure boundary tube bypass path.

TABLE 9. HEAVY WATER/LIGHT WATER INTERFACE LEVELS THROUGHOUT THE REACTOR AS A FUNCTION OF TIME

		Interface Level (m) (0.881 m = Bottom of Lower Core)[a]			
Time Point	Time (s)	Lower Core Flow Path	Upper Core Flow Path	U. C. Bypass	Central Hole
1	0.0	0.88100	0.87395	-	0.70480
2	0.011742	1.20273	1.01955	-	0.82222
3	0.023484	1.43417	1.16515	-	0.93964
4	0.035226	1.58447	1.31075	-	1.05706
5	0.046968	1.73477	1.51846	1.46712	1.17448
6	0.058710	1.88506	1.84019	1.64325	1.29190
7	0.070452	2.03535	2.02046	1.81938	1.40932
8	0.082194	2.18564	2.18133	1.99551	1.52674
9	0.093936	2.33593	2.34219	2.17164	1.64416
10	0.105678	2.48622	2.50306	2.34777	1.76158
11	0.117420	2.63651	2.66392	2.52390	1.87900

a. See Figure 3 for a better understanding of these levels.

The analysis covers the period from the time the interface reached the bottom of the lower core heated length until the time the interface in the central hole region reached the elevation of the top of the upper core heated length. This period of interest, 0.11742 s, was subdivided into ten equal intervals, and the interface levels in each of the flow paths

were calculated at each of the 11 time points. Results of the calculations are provided in Table 9. The interface levels in all regions are referenced to the elevation where the core inlet flow is divided among the flow paths, 0.881 m below the bottom of the lower core. For better visualization of the event, sketches were made of the fluid conditions at the first three time points and are shown in Figure 3.

Table 10 presents the core multiplication factor for the reference core with heavy water and for each of the three time steps during light water ingress. The reactivity drops as the light water enters and comes up to the bottom of the inner fuel element. This occurs because large amounts of light water absorb many more thermal neutrons than heavy water. The reactivity increases as the light water moderates more neutrons in the fuel region. The reactivity then drops again as the effect of neutron absorption becomes more important than the effect of moderation. The reactivity continues to drop after 0.0235 s. Several dollars worth of reactivity entering the core in 0.02 s would be a great safety concern. However, it is unlikely that the light/heavy-water interface would be well-defined, non-degrading, or flat.

TABLE 10. THE REACTIVITY EFFECT OF A SUDDEN INGRESS OF LIGHT WATER FOR THE ANS OPERATING AT FULL POWER POWER WITH THE CONTROL RODS INSERTED TO CORE MIDPLANE

Case	Core Multiplication Factor	Core Reactivity (%Δk/k)
Reference	1.0306	0.0
t = 0.0 s	1.0003	-2.98
t = 0.0117 s	1.0897	+5.58
t = 0.0235 s	1.0367	+0.59

A front of light water somehow entering the core during full power operation would result in a sudden positive reactivity insertion. Adding dilute amounts of H_2O in the primary coolant system and in the reflector tank are probably more realistic cases than a non-mixing front of light

water. When light water enters the reflector tank, the core reactivity drops as shown in Table 11. Thus any transfer of light water from the light water pool (biological shield surrounding the heavy water tank) to the heavy water tank will reduce core reactivity.

TABLE 11. THE EFFECT OF DILUTE LIGHT WATER INGRESS INTO THE REFLECTOR TANK ON THE CORE REACTIVITY

Percent H_2O in Tank	Percent Reactivity Change from 100% D_2O
1	- 2.72
10	-14.09
20	-18.85

Light water could also leak into the primary coolant system after the depressurization that would follow a pipe break. Reactor control rods would be inserted during the low pressure reactor scram, but we have not taken this into account. The light water would probably mix well with the heavy water. Therefore, we replaced the heavy water everywhere inside the core pressure boundary tube (CPBT) with various mixtures of light and heavy water. Figure 4 shows the effects of these mixtures on the core reactivity and the peak thermal neutron flux in the reflector. A maximum of about 3.3 $ or 2.4% reactivity could be inserted during a light water ingress accident with significant mixing. This ignores any movement of control and safety rods to compensate. The core multiplication factor is highest with about 15% H_2O and 85% D_2O inside the CPBT. This occurs mainly because the fuel is greatly undermoderated from the coolant channels, and the introduction of H_2O improves the moderation. However, above 15% H_2O, the H_2O surrounding the fuel elements acts as a poison and begins to overwhelm the effect of increasing moderation inside the fuel element. The peak thermal neutron flux in the reflector decreases as the percent of H_2O increases because H_2O absorbs more neutrons than D_2O.

For the analysis presented in Figure 4, control rods were assumed to maintain a constant position above the core midplane in the central hole region of the PDQ model (i.e., no credit was taken for reactor scram).

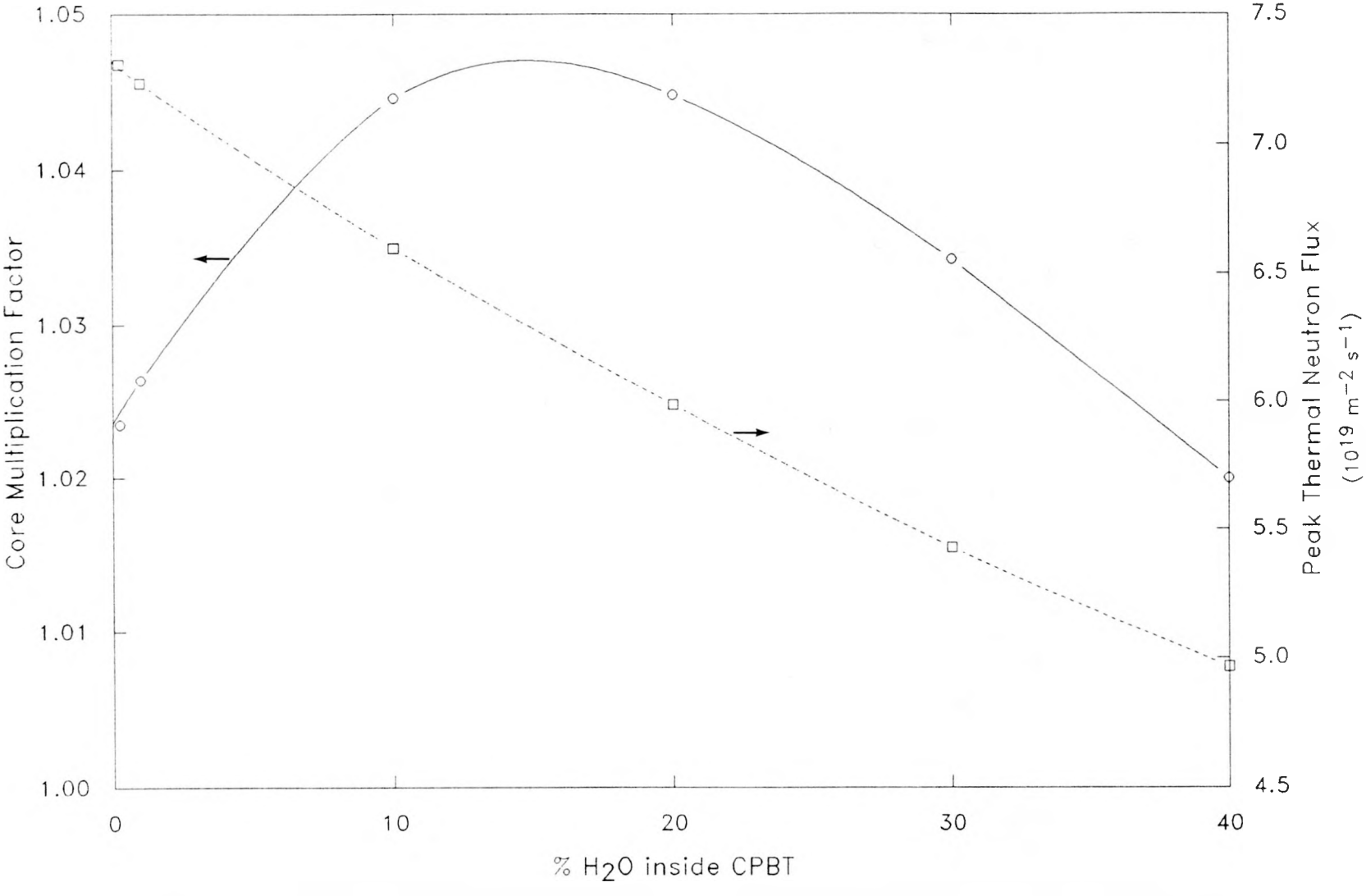

Figure 4. The core multiplication factor is highest when there is about 15% H_2O and 85% D_2O inside the core pressure boundary tube. The peak thermal neutron flux in the reflector decreases as the percent of H_2O increases.

Because the nuclear cross sections for this region are homogenized and transport-corrected, we did not insert any H_2O into this region. Therefore, the effect of the spectrum shift on the control rod worths has not been included. However, one PDQ prediction was compared with the three-dimensional MCNP model with the control rods and H_2O/D_2O mixture represented explicitly in the central hole.

In the MCNP model, we replaced heavy water everywhere inside the core pressure boundary tube with a mixture of 20% H_2O and 80% D_2O. Control rods were located at core midplane to be consistent with the PDQ model. MCNP predicts a 2.37% increase in core reactivity with the 20% H_2O/80% D_2O mixture because of the improved neutron moderation. This compares very well with the PDQ prediction of a 2.04% reactivity increase. Thus MCNP confirms the PDQ calculations. As the control system design evolves, we will include the effect of control rod motion in these calculations. We expect that the negative reactivity insertion from the control system will occur faster than the positive reactivity insertion from the light water.

Several methods for reducing the reactivity impact of light water have been suggested. Soluble boron poison could be added to the light water in the pool that surrounds the heavy water tank. Any light water ingress would then reduce core reactivity. During normal operation, boron in the light water pool does not significantly affect core reactivity. The boron may also improve the shielding aspects of the pool. However, soluble boron in the light water may be unacceptable if flux level instruments must be located in the pool. One solution is to eliminate or reduce the possibility of sudden light water ingress into the high pressure primary system. Another solution is to operate the primary system with 15% H_2O and 85% D_2O, although this would reduce the peak thermal neutron flux by about 14%. Burnable boron poison could be distributed throughout the fuel instead of only in the fuel plate end caps. During light water ingress the fuel spectrum softens, which would lead to greater absorption in the boron. Similarly, the addition of U-238 to the fuel may improve the safety. The flow distribution into the core could be modified to delay the coolant entering the coolant channels. If the coolant entered the

central hole first, the extra absorption in the light water would help compensate for a positive reactivity insertion in the fuel. Study of these methods, which could lead to a reactor design that eliminates reactivity insertion under any credible scenario of light water ingress, will continue.

6. SINGLE FUEL ELEMENT CRITICALITY

The PDQ-7 code was used to analyze fresh and exposed single fuel elements surrounded by heavy water or light water. Burnable boron poison was present in the fuel plate end caps at the beginning of cycle. Table 12 lists the core multiplication factors for these cases. The elements are each supercritical in heavy water and subcritical in light water. This occurs mainly because the element geometry was optimized for heavy water, and not light water. Light water in the large inner holes of the fuel elements acts as a poison. Therefore, transportation of fresh fuel elements is not a major problem from the standpoint of a fuel shipment cask falling into a river. However, extreme caution is required when handling fresh elements in the vicinity of heavy water. Some control poison mechanism must be in place when loading the fuel elements. This could be a boron shroud around the outside and/or inside of each element, or boron plates inserted into the coolant channels during fuel loading. In addition, this poison mechanism must be in place when removing elements from the core.

TABLE 12. MULTIPLICATION FACTORS FOR FRESH SINGLE FUEL ELEMENTS SURROUNDED BY HEAVY WATER OR LIGHT WATER

	Heavy Water	Light Water
Upper fuel element	1.2326	0.8056
Lower fuel element	1.1295	0.8391

The exposed fuel element results in Table 13 indicate that the upper element will be supercritical at end-of-cycle (EOC) if dropped in a large

pool of D_2O. The structure surrounding the fuel element has a large negative reactivity worth. In addition, burnable boron poison, which has a large negative reactivity worth at the beginning-of-cycle, is essentially gone by the end of cycle, increasing the element reactivity. The multiplication factor increases as the xenon decays several days after the reactor shutdown. Thus, special care is required during refueling. Some sort of control poison must be present around the spent fuel until the fuel is safely stored in a light water pool.

TABLE 13. SINGLE FUEL ELEMENT MULTIPLICATION FACTORS WITH END-OF-CYCLE CONCENTRATIONS WHEN SURROUNDED ONLY BY HEAVY WATER

Concentrations at 14 days	Element Multiplication Factor	
	Upper Element	Lower Element
with Xe-135	1.1855	0.9301
without Xe-135	1.2399	0.9692

7. FUEL ELEMENT MOVEMENT

The reactivity effect associated with the axial alignment of the fuel elements has been investigated. We evaluated the reactivity effect of fuel element movement to identify the potential reactivity insertion that could be obtained from fuel collapse. We have not performed any calculations that show the shape of a collapsing fuel element. As a crude approximation, we have looked at the case where the lower fuel element moves up until it is aligned with the upper fuel element. The fuel element is assumed to maintain its shape and U-235 distribution during the upward collapse. Although this is physically impossible because the fuel elements actually have different side plates, we assume that both elements share a common side plate during the collapse, and the extra Al-6061 is simply removed from the problem. The Al-6061 associated with the target spaces is also removed as the lower element collapses.

The intent of this study is to provide approximate values for reactivity insertion for the preconceptual core, and then later provide

more accurate values for the conceptual core. We did not examine several intermediate steps during the element collapse. Setting up a completely new mesh structure for each step is very time consuming. Therefore, we did not determine the point of maximum reactivity.

The four-group diffusion theory code PDQ-7 was used to compute the effects of fuel element axial movement presented in Table 14. As the fuel elements are separated axially from the final preconceptual reference core design, the core multiplication factor decreases. As the fuel elements are brought together axially, such that they share one of the aluminum side plates, the core multiplication factor increases and then eventually decreases significantly. We are not sure exactly where this peak core multiplication factor occurs. However, the core reactivity could increase initially as the lower fuel element collapses upward. More detailed investigation will be required to analyze fuel element movement in the conceptual core.

TABLE 14. REACTIVITY WORTH OF FUEL ELEMENT AXIAL MOVEMENT AT BEGINNING OF CYCLE WITHOUT CONTROL RODS

Axial Separation (mm)[a]	Core Multiplication Factor
-494[b]	1.092
16	1.164
30[c]	1.161
60	1.153
120	1.139

a. Axial distance from the bottom of the outer element end caps to the top of the inner element end caps.
b. Both elements are aligned like a single core.
c. Preconceptual reference design.

The core multiplication factor decreases as the elements are pulled apart from some optimum position because the elements become less coupled and begin to have the properties of single elements. As the elements are brought together into complete alignment, the core multiplication factor also decreases because the elements are shielding each other from the thermal neutrons coming from the reflector and central hole. This shielding effect results in an average fuel spectrum that is much harder

for the single core than for the reference core. In our models, we did not reassign any U-235 cross section sets for the values presented in Table 14 to account for this shift in fuel spectrum. Therefore, we set up an MCNP model of the single core to verify the parameters computed with PDQ.

We set up an MCNP model of this single core to provide a better representation of the harder neutron spectrum in the fuel and to verify the parameters computed with PDQ. The MCNP model contains 15 kg of U-235. To be consistent with the PDQ model, the Al-6061 in the lower fuel element and the irradiation target regions were removed, and the control rods were fully withdrawn in the model.

The MCNP-calculated core multiplication factors are compared with the PDQ values in Table 15. MCNP and PDQ both predict a drop in the core multiplication factor close to 6% in going from the reference core to the single core. Thus, the PDQ results are reasonably accurate even though we did not recompute all the cross sections.

TABLE 15. REACTIVITY WORTH OF THE REFERENCE CORE AND SINGLE CORE AT BEGINNING OF CYCLE WITH CONTROL RODS OUT

Code	Core Multiplication Factor		Reactivity Difference (%)
	Single	Reference	
PDQ	1.092	1.161	-6.13
MCNP	1.0503 $\pm$ 0.0039	1.1205 $\pm$ 0.0045	-6.47

8. NEUTRON BEAM TUBE FLOODING

The sudden flooding of four beam tubes in the reflector has been estimated with MCNP. Table 16 compares two studies, one with and one without the beam tubes. These values indicate that the presence of beam

tubes does not have a large effect on reactivity. Probably only one beam tube would flood during an accident, resulting in a small positive reactivity insertion of about 0.13$. More detailed beam tube models will be developed with MCNP and run longer on the computer to improve the statistics.

TABLE 16. THE EFFECT ON REACTIVITY DUE TO INSERTING FOUR BEAM TUBES

Description	Core Multiplication Factor
No beam tubes	1.1343 ± 0.0044
4 beam tubes	1.1302 ± 0.0033

9. REFERENCES

1. C. D. WEST, "Overview of the ANS Project," Trans. Am. Nucl. Soc., 57, 288 (1988).

2. C. D. WEST, "The Advanced Neutron Source Facility: A New User Facility for Neutron Research," Proc. Int. Reactor Physics Conf., Jackson, WY, September 18-22, 1988, Vol. II, p. 155 (1988).

3. G. L. COPELAND, et al., "Advanced Neutron Source Final Preconceptual Reference Core Design," ORNL/TM-11234, Oak Ridge National Laboratory (1989).

4. J. R. BUCHANAN et al., "Report of the Advanced Neutron Source (ANS) Safety Workshop," CONF-8810193, Oak Ridge National Laboratory (1988).

5. J. M. RYSKAMP, F. C. DIFILIPPO, and R. T. PRIMM III, "Reactor Physics Methods for the Preconceptual Core Design of the Advanced Neutron Source," Trans. Am. Nucl. Soc., 57, 290 (1988).

6. R. A. GRIMESEY, D. W. NIGG, and R. L. CURTIS, "COMBINE/PC-A Portable ENDF/B Version 5 Neutron Spectrum and Cross Section Generation Program," NRRT-N-89-014, Idaho National Engineering Laboratory (1989).

7. C. J. PFEIFER, "PDQ-7 Reference Manual II," WAPD-TM-947(2), Westinghouse Atomic Power Division (1971).

8. J. F. BRIESMEISTER, Ed., "MCNP - A General Monte Carlo Code for Neutron and Photon Transport," LA-7396-M, Rev. 2, Los Alamos National Laboratory (1986).

9. E. L. REDMOND II and J. M. RYSKAMP, "Monte Carlo Methods, Models, and Applications for the Advanced Neutron Source," Trans. Am. Nucl. Soc., to be published (1990).

10. E. L. REDMOND II "Monte Carlo Methods, Models, and Applications for the Advanced Neutron Source," Masters Thesis, Massachusetts Institute of Technology (1990).

11. V. H. RANSOM, et al., "RELAP5/MOD2 Code Manual," NUREG/CR-4312, EGG-2396, Idaho National Engineering Laboratory (1985).

12. C. D. FLETCHER, A. E. RUGGLES, and N. C. J. CHEN, "Advanced Neutron Source System Modeling Using RELAP5," Trans. Am. Nucl. Soc., to be published (1990).